

Disruption of the nonneuronal *tph1* gene demonstrates the importance of peripheral serotonin in cardiac function

Francine Côté*, Etienne Thévenot*, Cécile Fligny*, Yves Fromes†, Michèle Darmon‡, Marie-Anne Ripoché§, Elisa Bayard*, Naima Hanoun‡, Françoise Saurini‡, Philippe Lechat¶, Luisa Dandolo§, Michel Hamon‡, Jacques Mallet*||, and Guilain Vodjdani*

*Laboratoire de Génétique Moléculaire de la Neurotransmission et des Processus Neurodégénératifs, Centre National de la Recherche Scientifique, Unité Mixte de Recherche 7091 et Institut Fédératif de Recherche 70 (Neurosciences), Bâtiment CERVI, Hôpital de la Pitié-Salpêtrière, 83, Boulevard de l'Hôpital, 75013 Paris, France; †Institut de Myologie et Institut Fédératif de Recherche 14 (Coeur, Muscle, Vaisseaux), Institut National de la Santé et de la Recherche Médicale Unité 582, Centre Hospitalier Universitaire Pitié-Salpêtrière, 47, Boulevard de l'Hôpital, 75013 Paris, France; ‡Laboratoire de Neuropsychopharmacologie, Institut National de la Santé et de la Recherche Médicale, Unité 288, et Institut Fédératif de Recherche 70 (Neurosciences), Centre Hospitalier Universitaire Pitié-Salpêtrière, 91, Boulevard de l'Hôpital, 75013 Paris, France; §Genomic Imprinting Group, Génétique, Département Développement et Pathologie Moléculaire, Institut Cochin, 24, Rue du Fbg St Jacques, 75014 Paris, France; and ¶Service de Pharmacologie, Unité Propre de Recherche de l'Enseignement Supérieur 2391 et Institut Fédératif de Recherche 14 (CMV), Centre Hospitalier Universitaire Pitié-Salpêtrière, 47, Boulevard de l'Hôpital, 75013 Paris, France

Edited by Floyd E. Bloom, The Scripps Research Institute, La Jolla, CA, and approved September 4, 2003 (received for review May 21, 2003)

Serotonin (5-HT) controls a wide range of biological functions. In the brain, its implication as a neurotransmitter and in the control of behavioral traits has been largely documented. At the periphery, its modulatory role in physiological processes, such as the cardiovascular function, is still poorly understood. The rate-limiting enzyme of 5-HT synthesis, tryptophan hydroxylase (TPH), is encoded by two genes, the well characterized *tph1* gene and a recently identified *tph2* gene. In this article, based on the study of a mutant mouse in which the *tph1* gene has been inactivated by replacement with the β -galactosidase gene, we establish that the neuronal *tph2* is expressed in neurons of the raphe nuclei and of the myenteric plexus, whereas the nonneuronal *tph1*, as detected by β -galactosidase expression, is in the pineal gland and the enterochromaffin cells. Anatomic examination of the mutant mice revealed larger heart sizes than in wild-type mice. Histological investigation indicates that the primary structure of the heart muscle is not affected. Hemodynamic analyses demonstrate abnormal cardiac activity, which ultimately leads to heart failure of the mutant animals. This report links loss of *tph1* gene expression, and thus of peripheral 5-HT, to a cardiac dysfunction phenotype. The *tph1*^{-/-} mutant may be valuable for investigating cardiovascular dysfunction observed in heart failure in humans.

Serotonin (5-hydroxytryptamine, 5-HT) was discovered in blood as a vasoconstrictor of large vessels (1). Subsequently, it has been found in the gastrointestinal tract as a contractile substance identical with enteramine (2), in the CNS as a neurotransmitter (3), and in the pineal gland as an intermediate in the synthesis of melatonin, the neurohormone implicated in the circadian rhythmicity of physiological functions (4). 5-HT is detected early during brain development, suggesting its involvement in neuronal proliferation, migration, and differentiation (5). 5-HT modulates a variety of behavioral functions, including regulation of sleep/wakefulness, appetite, nociception, mood, stress, and maternal or sexual behavior (6). Altered regulation of 5-HT in human affects behavioral traits and personality disorders, such as impulsive aggression, manic depressive illness, anxiety and alcoholism, and neurological conditions, such as migraine (7–10).

About 95% of the 5-HT in the periphery is in the gastrointestinal tract (11), where it initiates responses as diverse as nausea, intestinal secretion, and peristalsis and has been implicated in gastroenteric diseases, such as irritable bowel syndrome (12). The 5-HT originating from the gastrointestinal tract is stored in blood platelets and participates in blood coagulation and pressure and in homeostasis. In the heart, an increased 5-HT

availability has been shown to produce arrhythmia, leading to heart block or to valvular fibroplasia (13). 5-HT has also been suggested to regulate cardiovascular development (14). Recently, disruption of 5HT-2B receptor revealed a role for 5-HT by means of this receptor in heart morphogenesis (15).

At least 15 5-HT receptor subtypes are found in almost all tissues (16–18). All subtypes are present in the brain, although the 5HT4 receptor is predominantly found in the gut and the 5HT2B subtype, in the heart and stomach fundus (12, 15). A variety of molecules with agonistic or antagonistic action on the receptors have been used in studies of 5-HT functions, as have toxins and drugs affecting 5-HT synthesis (19, 20). However, the inherent toxicity of some of the molecules and the diverse side effects of others have limited such pharmacological investigations. Therefore, the mechanisms by which 5-HT is involved in these physiological processes are not completely understood.

The first step in the biosynthesis of 5-HT is catalyzed by tryptophan hydroxylase (TPH; EC 1.14.16.4), the rate-limiting enzyme of the pathway. TPH is thus the marker of 5-HT synthesis. The enzyme is present in four structures: the pineal gland, the serotonergic neurons in the raphe nuclei that project in all brain areas, the enterochromaffin cells, and the myenteric neurons in the gut (21, 22). TPH activity is modulated posttranscriptionally by phosphorylation (23–25), and protein isoforms from the brainstem and pineal gland, differing in physicochemical properties, have been identified possibly because of posttranscriptional events (26). The TPH cDNA was first isolated from rat pineal gland (27, 28) and used to study the regulated expression of the *tph* gene (29, 30). A diversity in TPH mRNA species from rats and humans has been revealed, which resides in length differences of the 3' or 5' untranslated regions (28, 31–33). Also, initial studies have shown that the level of TPH mRNA was 150 times more abundant in the pineal gland than in the raphe neurons, whereas the protein levels as analyzed by anti-TPH immunoreaction were similar (29, 30). The discrepancies between the amounts of mRNA and protein could result from the diversity in TPH mRNA species with differing translation efficiencies or stabilities or from the existence of a second gene (29). Based on *tph* gene inactivation, recent findings from

This paper was submitted directly (Track II) to the PNAS office.

Abbreviations: 5-HT, serotonin (5-hydroxytryptamine); TPH, tryptophan hydroxylase; ES, embryonic stem; β -gal, β -galactosidase; bpm, beats per minute; LV, left ventricle; ISH, *in situ* hybridization.

||To whom correspondence should be addressed. E-mail: mallet@infobiogen.fr.

© 2003 by The National Academy of Sciences of the USA

Walther and colleagues (34) and from our laboratory (unpublished data) have revealed the existence of a second *tph* gene (*tph2*).

In this article, we describe the consequences at the biochemical, histological, and physiological levels of the targeted disruption of the *tph1* gene and its replacement by the β -galactosidase (*\beta*-gal) gene. We establish the neuronal expression of *tph2* in the raphe nuclei and the myenteric plexus neurons and the nonneuronal expression of *tph1* in the pineal gland and the enterochromaffin cells. Most importantly, *tph1*^{-/-} mice are viable and fertile, yet they suffer progressive cardiopathy that leads to heart failure. These results reveal the importance of circulating 5-HT in the modulation of cardiovascular function.

Experimental Procedures

***tph1* Gene-Targeting Construct.** Two clones from a mouse 129/SvJ genomic library (Stratagene) were isolated. A 5.3-kb *Hind*III-*Xba*I fragment spanning exons 2 and 3 was used. By mutagenesis, a *Nco*I site was created at the initiation codon of exon 2, and a 4.6-kb *Bsp*HI nslacZneopolyA cassette (kindly provided by Niels Galjart, Medical Genetic Center, Erasmus University, Rotterdam) was inserted at this site. The TPH1-*lacZ* junction was confirmed to be in-frame by sequence analysis. A 4.7-kb *Eco*RI fragment containing exons 4, 5, and part of exon 6 was ligated to the 3' end of the construct.

Embryonic Stem (ES) Cell Culture and Generation of Chimeric Mice.

The targeting construct was linearized at the single *Not*I site, and electroporation was carried out as described (35). Neomycin selection was performed in a medium containing 360 μ g/ml of G418 (GIBCO/BRL) for 9 days. Isolated ES cell neoresistant colonies were transferred to 96-well dishes and divided in two for freezing and DNA analysis. Nine rounds of electroporation were performed, and \approx 3,000 ES cell clones were screened for the homologous recombination event. After the last round, one positive ES cell clone was obtained of 768 tested. The recombinant G6 clone was amplified and injected into C57/BL6 blastocysts that were then transplanted into pseudopregnant female mice. Male chimeras displayed efficient germ-line transmission. The targeted allele was bred to both C57/BL6 and 129SvJ mouse strain backgrounds.

Identification of Genotype. Genomic DNA was extracted from ES cells and mice tails and digested according to standard procedures (36). Southern blot analysis with *Eco*RI-digested genomic DNA were performed with a 5' 404-bp external fragment (Fig. 1A). The 5' probe hybridizes to an 8-kb fragment in wild-type DNA and to an additional 5.4-kb fragment in targeted DNA (Fig. 1B).

In Situ Hybridization (ISH). 3'-UTR sequences of *tph1* and *tph2* from position +1434 to +1675 and +1603 to +2539, respectively, and a fragment of *LacZ* gene (kindly provided by A. Guerci, Laboratoire de Génétique Moléculaire de la Neurotransmission et des Processus Neurodégénératifs, Paris) were used for riboprobe synthesis from 1 μ g of linearized plasmid in the presence of 3.5 nmol of digoxigenin-11-UTP by using the Riboprobe system kit (Promega). The primers used were the following: TPH1fw1434, 5'-TGATGGTTTCCAGTGCAT-ATCC-3'; TPH1rev1675, 5'-CGTGGCACGTGAAGTATATT-TC-3'; TPH2fw1603, 5'-CTAGAACCAGAGTTATTGTC-AGC-3'; TPH2rev2539, 5'-CTACAGTAGACTTGTCAG-ATGTC-3'; LacZ1, 5'-ACCTGGCGTTACCCAACCTA-ATCG-3'; LacZ4, 5'-GCGTACTGTGAGCCAGAGTT-3'. ISH was performed as described (37) by using sense and antisense riboprobes on 250- μ m-thick serial sections.

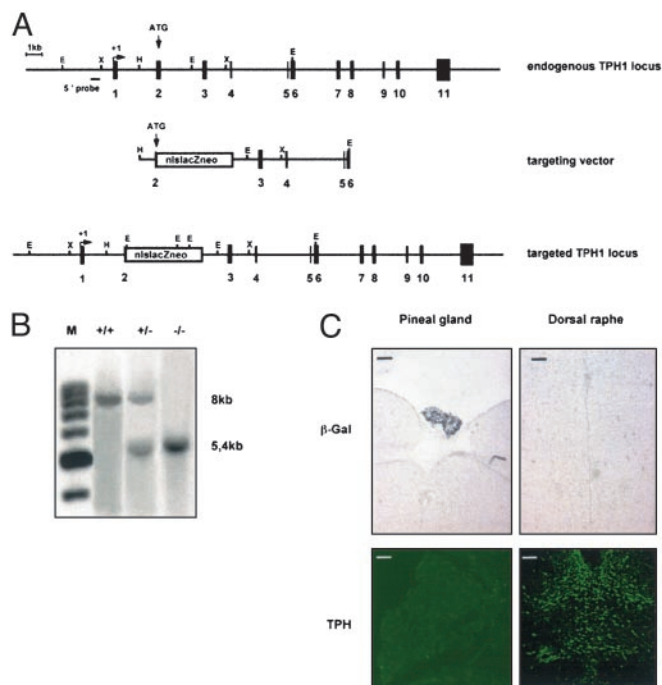


Fig. 1. Targeted disruption of the *tph1* gene. (A) Strategy for targeting the *tph* gene. (Top) The endogenous *tph1* locus. (Middle) The targeting construct. (Bottom) The structure after homologous recombination. (B) Southern blot analysis of the wild-type (+/+), heterozygous (+/-), and homozygous (-/-) alleles. The 5' probe, as indicated in A, recognizes a sequence outside the recombinant region. An 8-kb *Eco*RI fragment is detected in the wild-type allele, and a 5.4-kb fragment is detected in the recombinant allele. (C) Immunohistochemical analysis of the pineal gland and the dorsal raphe nucleus of homozygous *tph1* mutants. (Upper) β -Gal immunoreactivity. (Lower) TPH immunoreactivity as described (39). (Scale bars = 0.1 mm.)

Measurements of 5-HT and 5-Hydroxyindolacetic Acid Levels by HPLC.

Mutant mice and wild-type littermates were rapidly decapitated, and the organs were removed, weighed, and sonicated for 5 s in 10 volumes (vol/wt) of 0.1 N perchloric acid/0.05% disodium EDTA/0.05% sodium metabisulfite. 5-HT was extracted, and 10- μ l samples were injected onto a Beckman Ultrasphere 5- μ m IP column (Beckman) (38). Eluted 5-HT and 5-hydroxyindolacetic acid were quantified electrochemically (at 0.65 V) and concentrations were calculated in nanograms per gram of organ or nanograms per milliliter of blood.

Histological Analysis and Immunohistochemistry.

Deeply anesthetized animals were transcardially perfused with PBS and then 4% paraformaldehyde (PFA). The brains were removed, postfixed for 24 h in 4% PFA at 4°C, and transferred to 15% sucrose. Coronal sections (16 μ m thick) were cut with a freezing cryotome. Sections were immunolabeled for β -GAL or TPH (39). Hearts were removed and immersed in 4% PFA in PBS and embedded in paraffin. Transverse sections (5 μ m thick) were obtained from each heart and were stained with hematoxylin/eosin/saffron.

Hemodynamic Evaluation.

Twenty-week-old mice were anesthetized by i.p. injection of ketamine (50 mg/kg), xylazine (8 mg/kg), and midazolam (0.1 mg/kg). Spontaneous ventilation was maintained. The right carotid artery was dissected through a vertical cervicotomy. The distal end was ligated, and a conductance catheter (Millar Instruments, Houston, TX, model SPR-839) was inserted through the proximal end of the right carotid artery and positioned in the left ventricle (LV). After a brief period of stabilization, simultaneous LV pressure and LV

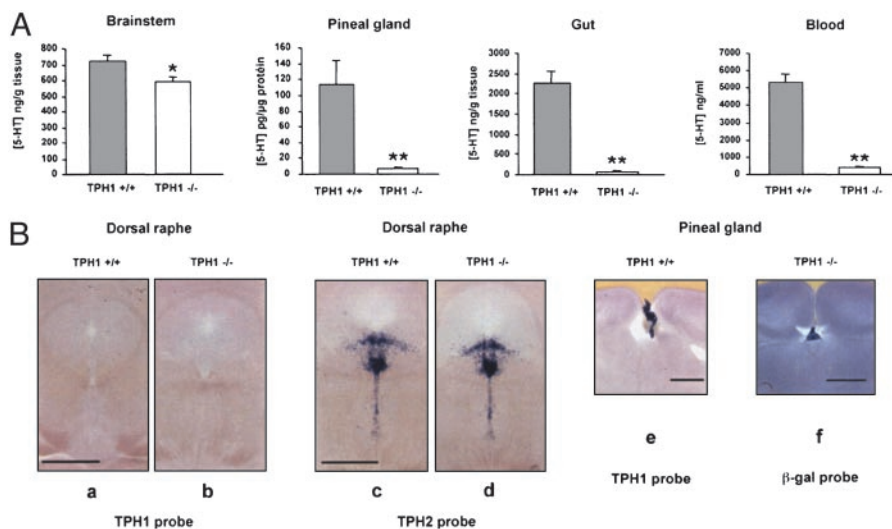


Fig. 2. Tissue-specific expression of *tph1* and *tph2*. (A) 5-HT levels in *tph1*^{-/-} and *tph1*^{+/+} mice in the brainstem (*tph1*^{-/-}, *n* = 11, and *tph1*^{+/+}, *n* = 8), the pineal gland (*tph1*^{-/-}, *n* = 17, and *tph1*^{+/+}, *n* = 8), the gut (*tph1*^{-/-}, *n* = 10, and *tph1*^{+/+}, *n* = 4), and the blood (*tph1*^{-/-}, *n* = 7, and *tph1*^{+/+}, *n* = 7). Values are expressed as mean ± SEM; *, *P* < 0.05; **, *P* < 0.001 (Student *t* test) for the difference between *tph1*^{-/-} and *tph1*^{+/+} mice. (B) TPH1 and TPH2 mRNAs as revealed by ISH. The TPH1 riboprobe was used in *Ba*, *Bb*, and *Be*; the TPH2 riboprobe was used in *Bc* and *Bd*. The β-GAL riboprobe was used in *Bf*. (Scale bars = 1 mm.)

volume were recorded at baseline. Contractility (dP/dt_{max}) and relaxation (dP/dt_{min}) were calculated as first-degree derivatives of the pressure. Pressure–volume loops were established by varying the load conditions of the LV through occlusion of the inferior vena cava. Volume load was obtained by i.v. injection of 200 μl of physiological serum, and differential measures were made. Finally, animals were killed by injection of excess anesthetic, and their hearts were harvested for histological analysis.

Results

Targeting of *tph1*, Germ-line Transmission of the Null Allele, and Analysis of TPH Expression in the Mutant Mice To define the *in vivo* action of 5-HT, we disrupted the *tph1* gene by homologous recombination in mouse R1 ES cells. The β-gal gene was knocked in the *tph* locus to follow expression in the TPH1-expressing sites. The design of the replacement vector was such that, in the construct, the translated portion of the first coding exon and the proximal part of the next intron of the *tph1* gene were substituted with an in-frame nuclear localized *lacZ* (nslacZ) gene and a neomycin-resistance (*neo*^r) selection cassette (Fig. 1A). Thus, the resulting targeted allele gives rise to a fusion protein consisting of 7 bp of the *tph1* gene followed by nslacZneo. After several rounds of electroporation with the targeting vector, one targeted ES cell clone was obtained of the 768 tested. By Southern blot analysis, the G6 clone was identified (Fig. 1B). Nine male mice were generated, five of which were highly chimeric and efficiently transmitted the null allele into the germ line. Heterozygous offspring were intercrossed to obtain homozygous *tph1*^{-/-} mice. Viable and fertile homozygous *tph1* mutant mice were born with the expected Mendelian frequency (*tph1*^{+/+}, 21.3%; *tph1*^{+/-}, 54%; *tph1*^{-/-}, 24.7%; *n* = 320).

We next tested for *tph1*-directed *lacZ* expression. The pineal gland of *tph1* null mice was strongly immunoreactive for β-GAL but not for TPH1 (Fig. 1C). The dorsal raphe nucleus of *tph1*^{-/-} mice was not immunoreactive for β-GAL but revealed a signal with the TPH antibodies used. This finding is very likely due to cross-immunoreactivity with the commonly used TPH antibodies.

5-HT concentration was determined in the organs where 5-HT synthesis is known to occur (Fig. 2A). 5-HT was slightly less abundant in the brainstem of mutant than in wild-type mice (*P* < 0.05), but it was very much less abundant in the gut (3.4% of wild-type) and blood (8%) and barely detectable in the pineal gland. In other organs, such as lung, heart, and kidney, the

remaining 5-HT levels ranged between 8% and 11% of wild-type level. No differences were observed between male and female mice. *tph1*^{-/-} mouse gut contains only 3.4% of the 5-HT found in *tph1*^{+/+} gut, presumably originating from the myenteric serotonergic neurons. Because these neurons are mainly located in the duodenal portion of the gut, we then measured the 5-HT concentration from the duodenum and the jejunum separately. As expected, very little 5-HT was found in the jejunum of *tph1*^{-/-} mice (0.7%), whereas in the duodenum the level of remaining 5-HT was similar to that found in the whole gut (3.4%) of *tph1*^{-/-} mice (data not shown).

Tissue-Specific Expression of TPH1 and TPH2. The distribution of TPH1 and TPH2 mRNAs was studied by ISH in known sites of 5-HT synthesis both in wild-type and *tph1*^{-/-} mice. The TPH1 and TPH2 probes used in this work were specifically designed to avoid any cross-hybridization. TPH1- and TPH2-specific 3'-UTR probes and a β-GAL probe were used either in the antisense strand for mRNA detection or in the sense strand as control. No TPH1 mRNA (Fig. 2B *a* and *b*) or β-GAL mRNA (not shown) were detected in the dorsal raphe nucleus of wild-type or mutant animals. The slight 5-HT reduction (as shown on Fig. 2A) may thus be caused by the decreased amount of circulating 5-HT. TPH2 mRNA was present in both wild-type and mutant dorsal raphe nuclei, and the loss of TPH1 expression in *tph1*^{-/-} mice did not lead to compensatory overexpression of TPH2 (Fig. 2B *c* and *d*). TPH1 mRNA was abundant in the pineal gland of wild-type mice, whereas β-GAL mRNA was abundant in the pineal gland of mutant mice (Fig. 2B *e* and *f*). TPH2 mRNA was not detected in the pineal gland of either wild-type or mutant mice (data not shown). In previous studies in the raphe neurons, faint signals were detected after long-exposure times and were attributed to be TPH1 mRNA (29, 30, 40). Our results show now that the signal was most likely due to cross-hybridization of the TPH1 probes, which, depending on the fragment used, could hybridize to the TPH2 messenger. The conditions we used clearly demonstrate the absence of TPH1 in the raphe nuclei and of TPH2 in the pineal gland. Furthermore, the ISH findings were confirmed by RT-PCR analysis of RNA from the brainstem and pineal gland by using specific 3'-UTR primers (data not shown). RT-PCR analysis was also used to confirm the inactivation of *tph1* in enterochromaffin cells. No

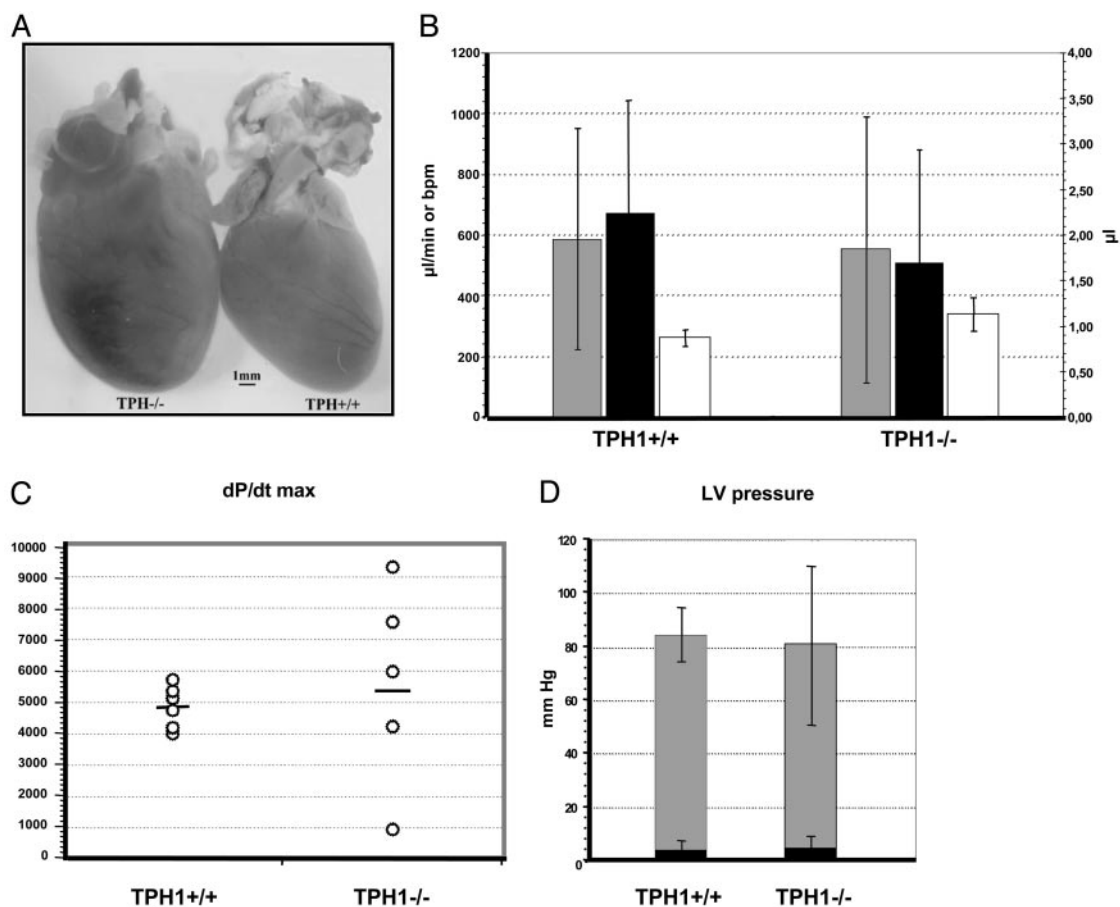


Fig. 3. Cardiac defect phenotype of homozygous *tph1* mutants. (A) Gross morphology of 26-week-old *tph1*^{-/-} and *tph1*^{+/+} mice. (Scale bars = 1 mm.) (B–D) Cardiac function of 20-week-old mice as assessed by *in vivo* cardiac catheterization. (B) The mean values of cardiac output (microliters per minute) (□), stroke volume (microliters) (■), and heart rates derived from the pressure input [beats per minute (bpm)] (□). Means for heart rate are: *tph1*^{+/+}, 266 ± 23 bpm; *tph1*^{-/-}, 336 ± 53 bpm; *n* = 6 and *P* = 0.007. (C) Distribution of individual *dP/dt*_{max} values measuring the maximum rate of the increase of the LV pressure. (D) Mean diastolic (■) and systolic (□) blood pressure as expressed in mmHg in the steady state (*n* = 6).

amplification product was detected in the gastrointestinal tract of *tph1*^{-/-} mice, whereas it is detected in the gastrointestinal tract of wild-type animals used as control. As an internal control of the experiment, an amplification product corresponding to GAPDH was detected (data not shown). Furthermore, an amplified RT-PCR product corresponding to TPH2 was obtained only from the duodenum of *tph1*^{-/-} or wild-type mice but not from the jejunum of these mice (data not shown). Thus, TPH2 supplies 5-HT to the brain and the myenteric plexus, whereas TPH1 supplies 5-HT to nonneuronal cells (enterochromaffin and pinealocytes).

***tph1*^{-/-} Mice Display Cardiac Abnormalities Without Structural Defects.** We studied the phenotypic consequences of a peripheral drop of 5-HT. *tph1*^{-/-} mice had breathing difficulties, progressive palor, and signs of fatigue reminiscent of blood-circulation abnormalities. In some mutant animals, heart size was larger (mean increase = 26%) than in wild-type littermates (Fig. 3A). Heart-to-body weight ratio was not significantly increased in the *tph1*^{-/-} mice (5.6 mg/g) as compared with wild-type mice (4.7 mg/g). Structural investigation of transverse sections of the heart showed no primary structural abnormalities indicative of developmental malformation (Fig. 4B). Histological examination of other organs, such as the kidney, adrenal gland, and lung, did not show any abnormalities, indicating that the pathological response to the drop of 5-HT appears specific to the heart. Hematoxylin/eosin/saffron staining did not show myocardial disarray or abnormal fibrosis in the ventricular myo-

cardium. The development and the structural integrity of the heart seemed to be unaffected by the lower level of circulating 5-HT.

To examine the hemodynamic profile of *tph1*^{-/-} mice, we performed cardiac catheterization to investigate LV function. In *tph1*^{-/-} mice, the mean values of cardiac output and stroke volume are decreased in the mutant mice as compared with wild-type littermates (Fig. 3B). Mean heart rate derived from the pressure input was significantly higher than that of control littermates (336 ± 53 vs. 266 ± 23, Fig. 3B) despite the influence of general anesthesia. However, an important variability is observed among the *tph1*^{-/-} animals that were analyzed. Heart rate of mutant mice ranged from 270 to 430 bpm, whereas the control animals ranged from 226 to 294 bpm. Mean systolic and diastolic LV blood pressures are not significantly different (Fig. 3D). Most notably, we observed again that individual data of LV systolic blood pressure in *tph1*^{-/-} mice displayed a large variability as compared with control animals. In the same way, mean end systolic pressure–volume relationship was 21 ± 9 and 20 ± 18 for the *tph1*^{+/+} and *tph1*^{-/-} mice, respectively, with no significant differences; however, a large variability occurred among individual values for *tph1*^{-/-} mice. The maximum rate of the increase of the LV pressure (*dP/dt*_{max}) of *tph1*^{-/-} mice was even more variable, although the mean value was not significantly different from that of control animals (Fig. 3C).

We report the parameters derived from the analysis of a series of loops obtained by altering the ventricular preload conditions in two extreme cases of *tph1*^{-/-} with *tph1*^{+/+} mice for reference. The

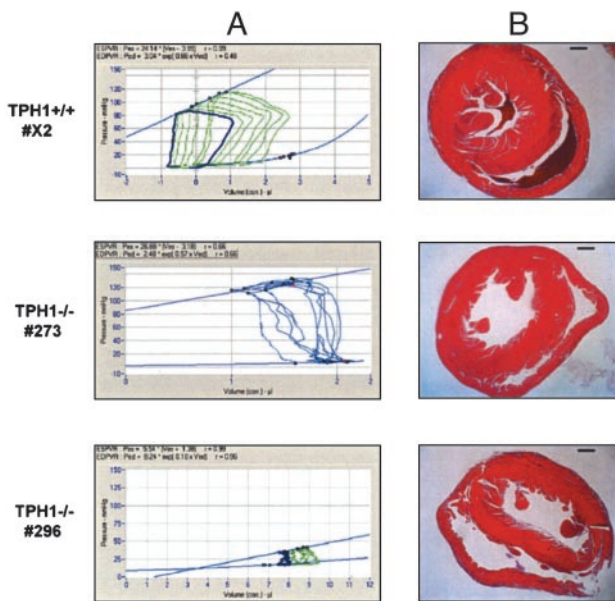


Fig. 4. Analysis of pressure–volume loops series and the histology of two *tph1*^{-/-} mutants representing extreme cases with a wild-type animal for reference (#X2). Mouse #273 compensates, and mouse #296 decompensates. (Scale bars = 1 mm.)

pressure–volume loops of these animals and the end systolic pressure–volume relationship revealed subnormal contractility in some cases and severe heart failure in others (Fig. 4A). Finally, the morphology of the ventricular myocardium correlated with the functional data. Two representative *tph1*^{-/-} mice with extreme features are illustrated (Fig. 4B): one (no. 273) had structurally normal myocardium and the other (no. 296) had dilated cardiac cavities. The mice lacking peripheral 5-HT did not show primary structural cardiac defects but presented functional alterations, which can progressively lead to heart failure.

Discussion

Our investigation of the *in vivo* role of 5-HT after targeted disruption of the *tph1* gene provides two important findings. First, *tph1* gene disruption leads to a dramatic loss of 5-HT from the periphery because of the absence of TPH expression in the enterochromaffin cells of the gut. Furthermore, we established, at the cellular level, the specific nonneuronal expression of TPH1 as compared with a neuronal expression of TPH2. Second, TPH1 null mice display an abnormal cardiac activity, which progressively leads to heart failure. This report links the loss of *tph1* gene expression and thus of peripheral 5-HT to a cardiac dysfunction. This loss does not affect the primary structure of the heart muscle.

In the *tph1*^{-/-} mice, the knockin of the β -gal reporter gene allowed us to monitor and map *tph1* gene expression. β -GAL was expressed in the pineal gland and enterochromaffin cells of the gut. TPH1 is thus the nonneuronal TPH isoform. In contrast, TPH2 is expressed exclusively in the neurons of the raphe nuclei and the myenteric plexus and, therefore, is the neuronal isoform. The two TPH proteins show an overall amino acid sequence identity of 65%; the identity is 83% in the catalytic domain (34). The N-terminal regions of the proteins are the most divergent; TPH2 is 42 aa longer than TPH1 in this region. This finding may account for some of the differences in physicochemical properties that have been determined (26). The *tph2* locus is near the *pah* locus encoding the phenylalanine hydroxylase on mouse chromosome 10, whereas the *tph1* and the *th* (tyrosine hydroxylase) loci are on chromosome 7. Thus, the aromatic amino acid hydroxylase genes may have arisen

from a common ancestor by gene duplication (41). Searches for other aromatic amino acid hydroxylase genes revealed no other gene encoding the same enzymatic function in mice. Therefore, unlike tyrosine hydroxylase and phenylalanine hydroxylase that are encoded by single genes, TPH activity is encoded by two genes that are, as it has been shown in this work, expressed in different organs and cells.

The concentration of 5-HT in the blood of *tph1*^{-/-} mice is 8% of the wild-type concentration. This concentration is due to the uptake and storage of 5-HT in the platelets. It may also be due to 5-HT from the raphe nuclei crossing the blood–brain barrier. It appears to be sufficient for development of the embryo and the viability of the mutants. *tph1*^{-/-} mice presented no visible developmental cardiac defect. Thus, either the 5-HT in the mutant is sufficient for organogenesis of the heart, or maternal 5-HT is supplied. Yavarone *et al.* (14) suggested that the 5-HT in mouse embryo is of maternal origin until at least embryonic day 10.

The TPH1 null mice suffer a progressive cardiovascular dysfunction leading to heart failure. However, no abnormalities in the morphology of the myocardium and no heart muscle remodeling occurred. Thus, this phenotype differs from other mouse models of heart defects involving the targeted disruption of genes encoding sarcomere or cytoskeletal proteins (reviewed in ref. 42). Disruption of the 5HT2B receptor causes embryonic or neonatal lethality because of heart morphogenetic defects (15). The surviving mutants exhibit thin ventricular walls caused by impaired proliferation of the myocytes and disorganized cytoarchitecture of sarcomeres within the compact zone and the myocardial trabeculae (15, 43). 5-HT seems to be involved by way of the 5HT2B receptor in regulating cardiac differentiation and proliferation during development and also in the cardiomyocyte structure of neonates. Pharmacological analysis also implicates 5-HT1A, 5HT2, 5HT3, 5HT4, and 5HT7 receptors in cardiovascular function. These receptors are located either on the nerve endings in the heart or on the myocardium, and their role still remains to be clarified (44, 45). Recently, it has been shown that 5-HT, through a direct stimulation of 5HT3 receptors on sympathetic afferents, participates in the activation of reflex responses. These are subsequent to an ischemic stress either at the abdominal or at the cardiac level (46, 47).

Cardiac function was assessed in *tph1*^{-/-} mice by examination of the hemodynamic profile. The beat/beat analysis of pressure and volume signals showed that maximum rate of increase in pressure during contraction (dP/dt_{max}) was much more variable between *tph1*^{-/-} mice than normal littermates. Also, despite the absence of significant differences of their mean values, other hemodynamic parameters, such as cardiac output, stroke volume, and end systolic pressure–volume relationship, display this variability among *tph1*^{-/-} animals as compared with the control. This finding may explain why mutant mice present a wide range in the severity of the heart-failure phenotype. The heart rate derived from the pressure input was significantly higher in *tph1*^{-/-} than in *tph1*^{+/+} mice. This finding appears to be a consequence of the slight decrease in cardiac output, which is partially due to the decreased stroke volume. Compensation of the hemodynamic performances might be frequency-dependent. Furthermore, no apparent difference in the LV end diastolic pressure was observed between the mutant and the wild-type mice. Therefore, the nature of the heart failure does not seem to have a diastolic origin.

The series of pressure–volume loops obtained by altering the ventricular preload conditions were analyzed. The end systolic pressure–volume relationship, which is relatively independent from the ventricular loading conditions, is a reliable index of the contractile state of the ventricle (48). It appears that the *tph1*^{-/-} mice initially are able to maintain near-normal contractility by a compensating phase. However, the chronic and profound decrease of peripheral 5-HT leads to progressive loss of heart contractility. The dilated heart loses its ability to adapt to the stress of the increased mechanical stretch that occurs during each heartbeat. A regulatory

role of the sympathetic system could provide an explanation of the cardiac dysfunction. The drop in the circulating 5-HT may lead to a decrease or lack of reflex stimulation by sensory nerves and thus result in a loss of contractility, such as that displayed by the *tph1*^{-/-} mice (49). Therefore, a decompensated state develops which leads to severe heart failure.

Heart failure is a syndrome resulting from the inability of the cardiac pump to meet the energy requirements of the body. It can originate from muscle abnormalities (review in ref. 50) or impairment of the energy metabolism and function of the muscle (review in ref. 51). These alterations can in turn be due to dysregulation of circulating factors, e.g., overdrive of the renin-angiotensin system. 5-HT can thus be considered as a significant circulating hormonal factor implicated in normal cardiovascular function either by acting directly on cardiomyocytes or by stimulating chemosensitive nerves from the heart. Thus, it appears that the level of circulating 5-HT is important, although the mechanisms and the signaling pathways by which 5-HT acts are not known. Treatment of embryos with selective antagonists of the 5HT2B receptor causes severe growth retardation, including a distended epicardial layer (52). The *tph1*^{-/-} mice appear to contain sufficient 5-HT for proper cardiac development and viability, but the amount in adults appears insufficient for normal cardiac function. Patients with carcinoid tumors have

high levels of 5-HT associated with arrhythmia, leading to heart block or to valvular fibroplasia (13). Also, mouse embryos grown in the presence of either a high concentration of 5-HT or 5-HT-specific reuptake inhibitors show a decreased proliferation of myocardium, cardiac mesenchyme, and endothelium (53).

In conclusion, the level of circulating 5-HT required for maintaining cardiovascular regulation is higher than that required for normal heart embryogenesis. The *tph1*^{-/-} mutant mouse may be a valuable model for cardiovascular defects associated with heart failure in humans (50). It also constitutes a valuable model for studying neural-myocardial interactions. Furthermore, it may become possible to develop TPH1-based therapy for cardiovascular diseases.

We thank H el ene Kiefer for expert assistance with the ISH. F.C. is the recipient of a postdoctoral fellowship from the Medical Research Council, Canada. E.T. is the recipient of a fellowship from La Fondation pour la Recherche M edicale. This work was supported by the Centre National de la Recherche Scientifique, Aventis, l'Institut de Recherche sur la Mo elle Epini ere, the University Pierre et Marie Curie, the Association Fran aise contre les Myopathies, the Conseil R egional d' Ile de France, the Institut National de la Sant e et de la Recherche M edicale, and Bristol-Myers Squibb Foundation (unrestricted biomedical research grant program).

- Rapport, M. M., Green, A. A. & Page, I. H. (1948) *Science* **108**, 329–330.
- Erspamer, V. & Asero, B. (1952) *Nature* **169**, 800–801.
- Dahlstrom, A. & Fuxe, K. (1964) *Acta Physiol. Scand.* **62**, 1–55.
- Reiter, R. J. (1991) *Endocr. Rev.* **12**, 151–180.
- Lauder, J. M. (1993) *Trends Neurosci.* **16**, 233–240.
- Jacobs, B. L. & Azmitia, E. C. (1992) *Physiol. Rev.* **72**, 165–229.
- Bellivier, F., Leboyer, M., Courtet, P., Buresi, C., Beaufile, B., Samolyk, D., Allilaire, J.-F., Feingold, J., Mallet, J. & Malafosse, A. (1998) *Arch. Gen. Psychiatry* **55**, 33–37.
- Lucki, I. (1998) *Biol. Psychiatry* **44**, 151–162.
- Mann, J. J., Brent, D. A. & Arango, V. (2001) *Neuropsychopharmacology* **24**, 467–477.
- Durham, P. L. & Russo, A. F. (2002) *Pharmacol. Ther.* **94**, 77–92.
- Gershon, M. D. (1999) *Aliment. Pharmacol. Ther.* **13**, 15–30.
- Kim, D.-Y. & Camillieri, M. (2000) *Am. J. Gastroenterol.* **95**, 2698–2709.
- Robiolio, P. A., Rigolin, V. H., Wilson, J. S., Harrison, J. K., Sanders, L. L., Bashore, T. M. & Feldman, J. M. (1995) *Circulation* **92**, 790–795.
- Yavarone, M. S., Shuey, D. L., Tamir, H., Sadler, T. W. & Lauder, J. M. (1993) *Teratology* **47**, 573–584.
- Nebigil, C. G., Choi, D.-S., Dierich, A., Hickel, P., Le Meur, M., Messaddeq, N., Launay, J.-M. & Maroteaux, L. (2000) *Proc. Natl. Acad. Sci. USA* **97**, 9508–9513.
- Saudou, F. & Hen, R. (1994) *Neurochem. Int.* **25**, 503–532.
- Stark, K. L., Oosting, R. S. & Hen, R. (1998) *Biol. Psychiatry* **44**, 163–168.
- Barnes, N. M. & Sharp, T. (1999) *Neuropharmacology* **38**, 1083–1152.
- Jouvet, M. (1999) *Neuropsychopharmacology* **21**, 24S–27S.
- Pineyro, G. & Blier, P. (1999) *Pharmacol. Rev.* **51**, 533–591.
- Lovenberg, W., Jequier, E. & Sjoerdsma, A. (1967) *Science* **155**, 217–219.
- Legay, C., Faudon, M., H ery, F. & Ternaux, J. P. (1983) *Neurochem. Int.* **5**, 721–727.
- Ehret, M., Pevet, P. & Maitre, M. (1991) *J. Neurochem.* **57**, 1516–1521.
- Makita, Y., Okuno, S. & Fujisawa, H. (1990) *FEBS Lett.* **268**, 185–188.
- Johansen, P. A., Jennings, I., Cotton, R. G. H. & Kuhn, D. M. (1996) *J. Neurochem.* **66**, 817–823.
- Kim, K. S., Wessel, T. C., Stone, D. M., Carver, C. H., Joh, T. H. & Park, D. H. (1991) *Mol. Brain Res.* **9**, 277–283.
- Darmon, M. C., Grima, B., Cash, C. D., Maitre, M. & Mallet, J. (1986) *FEBS Lett.* **206**, 43–46.
- Darmon, M. C., Guilbert, B., Leviel, V., Ehret, M., Maitre, M. & Mallet, J. (1988) *J. Neurochem.* **51**, 312–316.
- Dumas, S., Darmon, M. C., Delort, J. & Mallet, J. (1989) *J. Neurosci. Res.* **24**, 537–547.
- Hart, R. P., Yang, R., Riley, L. A. & Green, T. L. (1991) *Mol. Cell. Neurosci.* **2**, 71–77.
- Boulevard, S., Darmon, M. C. & Mallet, J. (1995) *J. Biol. Chem.* **270**, 3748–3756.
- Delort, J., Dumas, J.-B., Darmon, M. C. & Mallet, J. (1989) *Nucleic Acids Res.* **17**, 6439–6448.
- Wang, G.-A., Coon, S. L. & Kaufman, S. (1998) *J. Neurochem.* **71**, 1769–1772.
- Walther, D., Peter, J.-U., Bashammakh, S., H ortnagl, H., Voits, M., Fink, H. & Bader, M. (2003) *Science* **299**, 76.
- Ramirez-Solis, R., Davis, A. C. & Bradley, A. (1993) *Methods Enzymol.* **225**, 855–878.
- Sambrook, J., Fritsch, E. F. & Maniatis, T. (1989) *Molecular Cloning: A Laboratory Manual* (Cold Spring Harbor Lab. Press, Plainville, NY).
- Ravassard, P., Chatail, F., Mallet, J. & Icard-Liepkalns, C. (1997) *J. Neurosci. Res.* **48**, 146–158.
- Hamon, M., Fattaccini, C. M., Adrien, J., Gallissot, M. C., Martin, P. & Gozlan, H. (1988) *J. Pharmacol. Exp. Ther.* **246**, 745–752.
- Th evenot, E., C ot e, F., Colin, P., He, Y., Leblois, H., Perricaudet, M., Mallet, J. & Vodjdani, G. (2003) *Mol. Cell. Neurosci.* **24**, 139–147.
- Huh, S. O., Park, D. H., Cho, J. Y., Joh, T. H. & Son, J. H. (1994) *Brain Res. Mol. Brain Res.* **24**, 145–152.
- Craig, S. P., Buckle, V. J., Lamouroux, A., Mallet, J. & Craig, I. (1986) *Cytogenet. Cell Genet.* **56**, 157–159.
- Hoshijima, M. & Chien, K. R. (2002) *J. Clin. Invest.* **109**, 849–855.
- Nebigil, C. G., Hickel, P., Messaddeq, N., Vonesch, J.-L., Douchet, M. P., Monassier, L., Gy orgy, K., Matz, R., Andriantsitohaina, R., Manivet, P., et al. (2001) *Circulation* **103**, 2973–2979.
- Saxena, P. R. & Villalon, C. M. (1990) *J. Cardiovasc. Pharmacol.* **15**, S17–S34.
- Ramage, A. G. (2001) *Brain Res. Bull.* **56**, 425–439.
- Fu, L.-W. & Longhurst, J. C. (1998) *J. Physiol.* **509**, 729–740.
- Fu, L.-W. & Longhurst, J. C. (2002) *J. Physiol.* **544**, 897–912.
- Sunagawa, K., Maughan, W. L., Burkoff, D. & Sagawa, K. (1983) *Am. J. Physiol.* **245**, H773–H780.
- Fu, L.-W. & Longhurst, J. C. (2002) *Am. J. Physiol.* **282**, H100–H109.
- Chien, K. R. (2003) *J. Clin. Invest.* **111**, 175–178.
- Ventura-Clapier, R., De Souza, E. & Veksler, V. (2002) *News Physiol. Sci.* **17**, 191–196.
- Choi, D.-S., Ward, S. J., Messaddeq, N., Launay, J.-M. & Maroteaux, L. (1997) *Development (Cambridge, U.K.)* **124**, 1745–1755.
- Lauder, J. M., Tamir, H. & Sadler, T. W. (1988) *Development (Cambridge, U.K.)* **102**, 709–720.